

Wuerz Publishing Ltd

© Copyright 1993 by Wuerz Publishing Ltd

All rights reserved. No part of this book may be reproduced or transmitted in any form or by any means, electronic or mechanical, including photocopying, recording, or any information storage and retrieval system, without permission in writing from the publisher.

Mathematics Applied to Biology and Medicine
J Demongeot and V Capasso, editors

ISBN 0-920063-63-2

Printed in the United Kingdom

Recent Approaches to Immune Networks

Rob J. de Boer

Bioinformatics, University of Utrecht, Padualaan 8, 3584 CH Utrecht, The Netherlands

Avidan U. Neumann

Laboratoire de Physique Statistique de l'Ecole Normale Supérieure
24 rue Lhomond, F 75231 Paris Cédex 5, France, *and*, Physics Department,
Bar-Ilan University, Ramat-Gan IL-52100, Israel

Alan S. Perelson

Theoretical Biology and Biophysics, Theoretical Division
Los Alamos National Laboratory, Los Alamos, NM 87545, USA

Lee A. Segel

Department of Applied Mathematics and Computer Science, Weizmann Institute,
Rehovot IL-76100, Israel

Gérard Weisbuch

Laboratoire de Physique Statistique de l'Ecole Normale Supérieure 24 rue Lhomond,
F 75231 Paris Cédex 5, France

1. Introduction

Jerne (1974) proposed that the immune system has important network characteristics that are similar in many respects to neural networks. This paper outlines some recent approaches taken by the authors and their colleagues toward the analysis of immune networks. Other approaches have been omitted owing to space limitations, notably that of Coutinho, Stewart, and Varela (Stewart and Varela, 1991; Varela and Coutinho, 1991).

1.1. A minimal biological background

Pathogenic invaders, such as viruses or bacteria, provoke the immune system to

defend the body. The principal defenders are cells called *lymphocytes*. There are two main classes of such lymphocytes: B cells and T cells. Here we will consider simple situations in which T cells are ignored. We refer to De Boer and Hogeweg (1989c) for related models of T and B cell networks.

B cells can be subdivided into *clones*. All cells in a clone are identical. In particular these cells possess identical immunoglobulin receptor molecules that determine their specificity. Different clones are characterised by different antigen-combining sites on their receptors. If sufficient receptors on a cell form complexes with circulating molecules called *ligands*, then the cell can be triggered to secrete or proliferate. B cells secrete molecules called *antibodies* that are essentially identical in shape to their receptors. It is the central idea of network theory that it is not only the (*antigen*) molecules associated with invading pathogens that can stimulate B cells but all molecules with shapes complementary to the B cell receptors. Thus, for each lymphocyte there should be a set of antibodies, called anti-idiotypic antibodies, that should be able to bind the lymphocyte's receptors and stimulate the cell. Hence, for the time being, we will neglect antigens and assume that only antibodies can bind with lymphocyte's receptors.

1.2. A simple clonal network model

The different approaches outlined in this paper are based upon the model that was originally proposed by De Boer (1988) and De Boer and Hogeweg (1989a). The most crucial characteristic of this model is the bell-shaped activation function f . In this model $b_i(t)$ represents the population size of the i^{th} clone at time t , $i = 1, \dots, N$:

$$db_i / dt = m - db_i + pb_i f(h_i). \quad (1.1)$$

Here the constant m denotes the rate of supply of new cells from the bone marrow. The constant d denotes the death rate, so that an unstimulated cell has a lifetime of magnitude $1/d$. The *activation function* f denotes the fraction of cells that are proliferating, and p denotes the consequent proliferation rate. The influence of the exterior world on clone b_i is quantitated by the *field* h_i , which is assumed to be formed of a linear combination of the antibody concentrations A_j :

$$h_i = \sum_{j=1}^N K_{ij} b_j \quad (1.2)$$

The linear formula (1.2) may need to be refined in more accurate network theories.

In the simplest network models, the considerable simplification is made that every B cell is associated with a constant number A of antibody molecules. Then

$$h_i = \sum_{j=1}^N J_{ij} b_j \quad (1.3)$$

where $J_{ij} = AK_{ij}$

Specification of the interaction matrix J_{ij} poses a major modeling problem, for this specification determines the architecture of the immune network. In what follows, we will discuss the consequences of three different types of assumptions for characterising J_{ij} .

The activation function f is typically defined by

$$f(h_i) = \frac{h_i}{\theta_1 + h_i} \frac{\theta_2}{\theta_2 + h_i}, \quad (1.4)$$

where $\theta_1 \ll \theta_2$. Plotted as a function of $\log h_i$, the graph of $f(h_i)$ is a bell-shaped curve. An important argument for the use of a log bell-shaped function is that receptor cross-linking is involved in B cell activation. For ligands that are bivalent the cross-linking curve is bell-shaped and symmetric around its maximum (Perelson and DeLisi, 1980; Perelson, 1984).

2. A Cayley Tree Network

2.1. Classifying the attractors

The J_{ij} elements are computed by assuming that the network has the topology of a Cayley tree (Weisbuch, De Boer, and Perelson; 1990) with c connections per vertex (see Fig. 1). For reasons of simplicity the J_{ij} 's are chosen to be zero (no interaction) or one (maximum interaction). One clone in the network is assumed to react with antigen. This clone is chosen to be the root of the tree and is labelled b_1 . Under these conditions Eq. (1.3) reduces to

$$h_i = cb_2, \quad h_i = b_{i-1} + (c-1)b_{i+1}, \quad i \geq 2. \quad (2.1)$$

We consider the problem of classifying the different attractors of the network and interpreting the transitions from one attractor to another one under the influence of antigen. Let us start with the virgin configuration, corresponding to the hypothetical case where no antigen has been introduced and there is no internal stimulation of the network. Here all proliferation functions $f(h_i)$ are close to zero so that at steady state Eq. (1.1) implies $b_i = m/d$, for all i . After the introduction and elimination of an antigen, memory is obtained if some clones in the network reach stable level larger than m/d . We also require that when successive introductions of different antigens are made, the network remembers all these antigens. Memory of one antigen should be robust enough not to be destroyed by the introduction of another antigen. Such a scheme works if the response to any given antigen remains localised in the network.

In such a case, to each antigen there corresponds a patch of clones that are modified by the antigen. As long as patches corresponding to different antigens do not overlap, all antigens can be remembered. Once the idea of localised non-interacting attractors is accepted, everything is simplified. Instead of solving N equations corresponding to the immune repertoire, we only have to solve a small set of equations for the interacting clones in a patch.

2.1.1 . Immunity

Let us take as an example the case of an antigen reacting with b_1 that results in excitation of clones b_1 and b_2 but with clones b_3 remaining essentially at their virgin level (see Fig. 1,top). If one considers steady state solutions of Eq. (1.1) in

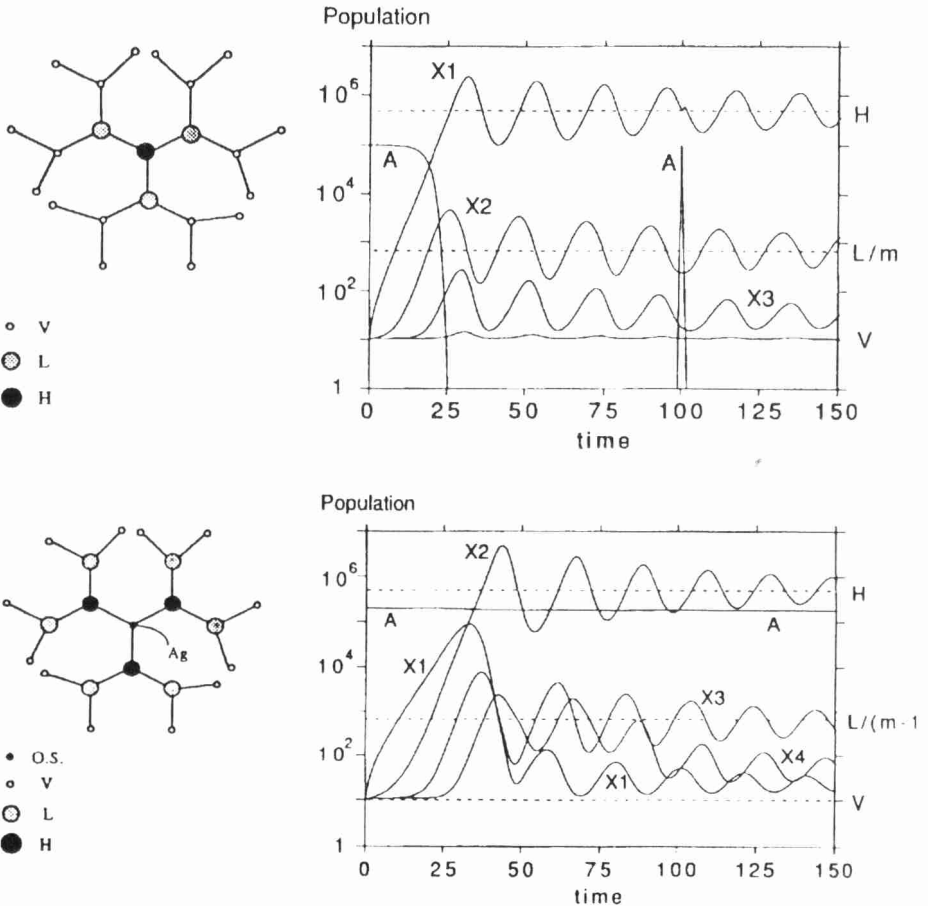


Fig.1. Two localised attractors of the immune network corresponding to immunity (top) and tolerance (bottom). Black circles correspond to large suppressive populations (of the order of θ_2), grey circles to medium excitatory populations (of the order of θ_1), and small white circles to small virgin or over suppressed

populations (of the order of m/d). The two graphs are time plots of the logarithm of the populations (numerical simulation results). A is antigen concentration. Immunity as a memory effect is illustrated in the plot at the top; a second antigen presentation with the same dose at time $t = 100$ results in a faster elimination than during the first presentation. Slow decay of large antigen concentration results in tolerance where a suppressive field acts on b_1 and prevents it from eliminating the antigen. GRIND software (De Boer, 1983) was used to generate Figs. 1 and 2.

which a large fraction of the cells are activated, i.e., $f(h_i) > 0$, the source m can be neglected and one expects steady state solutions when $f(h_i) = d/p$. For an immune system to be reactive, $p > d$, so that there will be two intersections of the line $y = d/p$ with the curve $y = f(h)$, one on each side of the maximum of the bell shaped curve. The fields below and above the maximum are called stimulatory and suppressive, respectively, since in the first case an increase in the field increases B cell proliferation, while in the second case such a change decreases the proliferation. One stable solution occurs when b_1 has a low stimulatory field and b_2 feels a high suppressive field (Weisbuch *et al.*, 1990). We expect a low stimulatory field solution, h_L , for b_1 and a large suppressive field solution, h_S , for b_2 . The field equations allow one to compute the populations:

$$h_1 = cb_2 = h_L \equiv \frac{d\theta_1}{p'}, \quad h_2 = b_1 + (c-1)\frac{m}{d} = h_S \equiv \frac{p'\theta_2}{d}, \quad (2.2a,b)$$

where $p' = p - d$. The solution remains localised only if the field h_3 on b_3 is much less than h_L ; otherwise b_3 would also proliferate:

$$h_3 = \frac{h_L}{c} + \frac{(c-1)m}{d} < h_L. \quad (2.3)$$

This is only possible if c is larger than one (i.e., multiple connectivity is essential to localisation) and if

$$\frac{p'cm}{d^2} < \theta_1. \quad (2.4)$$

This is equivalent to saying that the field due to c virgin clones should be insufficient to stimulate a clone.

2.1.2. Tolerance

Another localised attractor corresponds to tolerance (see Fig. 1, bottom). A strong suppressive field acts on b_1 due to b_2 ; b_2 populations proliferate due to a low field provided mainly by b_3 , b_3 populations remain low due to the suppressive field generated by b_2 , and b_4 populations remain nearly virgin (Weisbuch and Neumann, 1990). The field equations allow computation of the steady state populations:

$$h_2 = b_1 + (c - 1)b_3 = h_L = d\theta_1 / p'. \quad (2.5)$$

This gives b_3 by neglecting b_1 , which is small. With b_4 virgin

$$h_3 = b_2 + (c - 1)(m / d) = h_S = p'\theta_2 / d, \quad (2.6)$$

which gives b_2 . Then

$$h_1 = cb_2 \approx ch_S,$$

which, inserted in Eq. (1.1), shows that at steady state, b_1 is of the order of m/d , h_4 is small, and b_4 is nearly virgin.

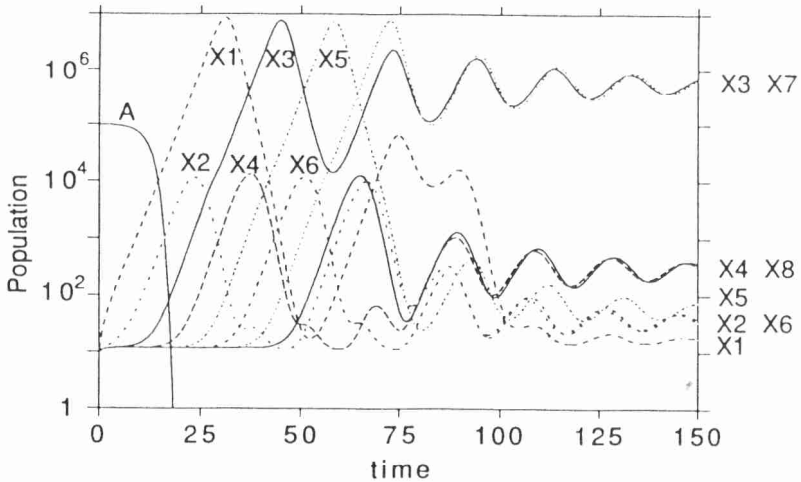


Fig.2. Time diagram for percolation. After antigen introduction, clones 1 and 2 return to virgin state, but clones 3,7,11,15,... are excited to the suppressive level. Clones 4,8,12,16,... sustain the excitation of 3,7,11,15,... .

2.1.3. Percolation

Some parameter sets allow excitation to propagate from the initial clones across all the network. In such a case percolation is observed, which corresponds to non-localised dynamics (Fig. 2). We do not expect percolation to be a normal condition, but it may appear in some diseases. We will argue in a future publication that this phenomenon may be relevant to *systemic lupus erythematosus* where a number of different autoantibodies are detected as if there were a type of percolation of the immune response.

2.2. Attaining the attractor: dynamics with antigen

Now that we have characterised the attractors, we would like to be able to predict which attractor is attained when antigen is injected into the system. We know from observation and experiment that, depending upon the age of the individual (foetal or adult) and the conditions of antigen introduction (high or low dose, presence or absence of adjuvant, intravenous or subcutaneous injections), immunity, tolerance or no response is obtained. In the model, antigen concentration y decreases because of the elimination proportional to the idiotypic clone b_1 :

$$d\gamma/dt = -k\gamma b_1 \quad (2.7)$$

The influence of the antigen on clone b_1 is taken into account by adding a new term in h_1 :

$$h_1 = cb_2 + \gamma \quad (2.8)$$

The nature of the attractors reached according to the parameters of the computer simulations are summarised in Fig. 3 (see Neumann and Weisbuch, 1991a). The kinetic constant k and the initial antigen concentration are the parameters that define antigen introduction. Theoretical analysis shows that they can be combined into a unique relevant parameter C defined as the b_1 concentration at the time of antigen elimination.

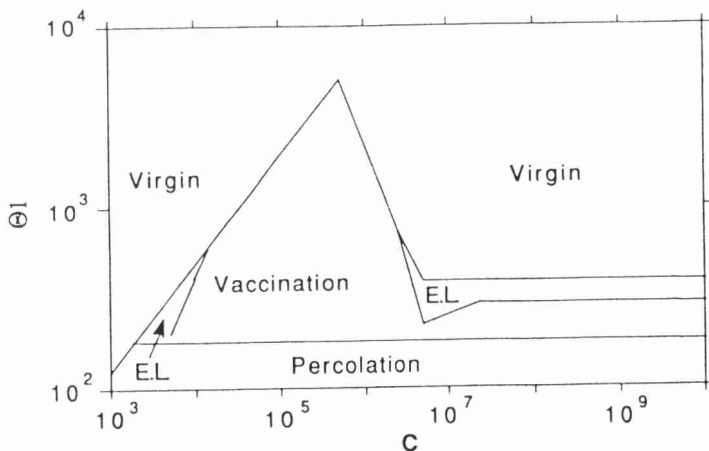


Fig.3 Diagram of the attractors attained by the dynamics as a function of θ_1 and C which parameterises antigenic stimulation.

By further simplifying the present model, one is able to derive the scaling laws that separate the different regimes in the parameter space (Neumann and Weisbuch, 1991a). The idea is to approximate the proliferation function $f(h)$ by a *window automaton*, a piecewise constant function that is one when the field h is between θ_1 and θ_2 , and zero otherwise. Populations excited from the virgin level then either exponentially decay or increase (with respective exponents d and $p - d$) according to the values of the field. The times between successive excitations can then be estimated and from them the transitions between regimes analytically computed.

2.3. Conclusions and Generalisations

We now have a simple model of the immune network, which exhibits rich dynamical behavior. In accordance with biological observations, the attractors reached under antigenic stimulation (immunity, tolerance, percolation) depend upon the conditions of the stimulation (dose, adjuvant, etc.) and upon the parameters of the network (to be related to the age of the animal). A comparison with neural nets, in their Hopfield (1982) version, for instance, reveals a similar approach to the analysis of attractors. Among differences, we might note the fact that in the immune nets the attractors are localised rather than distributed; that learning occurs by antigen introduction, which results in a local change of configuration of the attractor rather than a change of the J_{ij} 's; and that the memory capacity of the network varies as \sqrt{N} rather than N (Weisbuch, 1990).

We have tested whether this very simple scheme is generic for a larger class of networks. More elaborate versions of the simple Cayley tree model may allow for localised attractors:

- The introduction of loops into the network makes it necessary to generalise the condition for existence of localised attractors (Neumann and Weisbuch, 1991b). The immunity (tolerance, respectively) attractor only exists if the forward connectivity of the first (second) level of clones is larger than the backward connectivity of the third (fourth) level of clones. If the above condition holds, even loops do not change the dynamics qualitatively. Odd loops on the other hand, may favour either tolerance or immunity, depending on the level at which the odd loop exists.
- Using a continuous distribution of J_{ij} elements gives rise to avalanches (Neumann and Weisbuch, 1991b). In an avalanche percolation waves are launched repeatedly on all length scales of the network. Avalanches may be avoided by assuming that idiotypic interactions are negligible when the affinity is too low (see also De Boer *et al.*, 1992), or by assuming that suppression is less specific than stimulation (i.e., "long-range inhibition", see Segel and Perelson, 1988).
- The introduction of dynamics with different time scales for antibodies and B cells favours chaos (De Boer *et al.*, 1990), see also Section 4. But when the model is further refined to take into account the existence of lymphoid organs, the localised attractors may become stable again (Perelson and Weisbuch, 1991; De Boer, Kevrekidis, and Perelson, submitted).

3. The Shape Space Approach

We now turn to another approach to the specification of network architecture. This approach is based on exploiting the fact that the binding affinity of antibody and receptor molecules is determined by the degree of complementarity of their shapes (where shape includes related factors such as charge). It is reasonable to hope that five or ten shape measurements could provide a good approximation to binding affinity, yielding shape spaces of five to ten dimensions (Perelson and Oster, 1979). But to begin our discussion we will consider shape spaces of just one dimension. To fix ideas, the shape variable x can be thought of as the height of a wedge-shaped region that determines binding strengths, with positive x corresponding to a protuberance and negative x to an indentation. Perfect complementarity, and hence maximum binding affinity, occurs when the protuberance and the indentation are of the same length. For definiteness, the falling off of binding affinity for less complementary shapes is described by a Gaussian function of the distance between a given shape and its complement. This leads to the following field specification for clone b_i of shape $i \Delta$, where Δ is a constant:

$$h_i = \sum_{j=-\infty}^{\infty} g(i, j) b_j(t) \Delta . \quad (3.1)$$

Here

$$g(i, j) = G(2\pi\sigma^2)^{-\frac{1}{2}} \exp\left[-(i + j)^2 \Delta^2 / 2\sigma^2\right], \quad (3.2)$$

where G and σ are constants. Sometimes periodic boundary conditions are used. Alternatively, so-called *fixed boundary conditions* are employed, wherein clone sizes whose shapes lie outside a certain interval are fixed at zero magnitude.

An advantage of the shape space formalism is that the governing large system of ordinary differential equations, which formulate the dynamics of a discrete set of shapes, can readily be approximated by a few partial integro-differential equations in a continuous shape space. (See Segel and Perelson, 1988 - where, in fact, a first shape space model was originally postulated in continuous form.) Uniform solutions exist, for example the virgin state wherein the bone marrow source and cell death are in balance, in the absence of proliferation. The stability of these uniform states can be analysed by rather standard analytical methods. The stability results provide an important check on the numerical procedures that must be used to study the dynamics of the full problem. Moreover stability theory provides the framework for certain conceptual generalisations, notably the notion that an efficient immune system should possess a virgin state that is stable to infinitesimal perturbations (so that it does not explode when slightly stimulated) but is not too stable (so that it is controllable). See Segel and Perelson (1988) as well as De Boer, Segel, and Perelson (1992).

Simulations show that, except for sufficiently small disturbances to the virgin

state, even localised perturbations in shape space seem to grow until clones throughout shape space become excited. This is an example of the percolation phenomenon mentioned above. Other features of this type of simulation, such as plasticity of response and clonal organization, are discussed by De Boer *et al.* (1992).

Above, we discussed the hypothesis that immune memory is due to the attainment of a new steady state that remains after the antigenic challenge disappears. Most biologists, by contrast, would cite abundant evidence that memory is connected with the differentiation of special long-lived cells called *memory cells*. The two views of memory are not necessarily contradictory; both types of memory may co-exist. But even if memory is confined only to memory cells, network interactions must be taken into account. This is illustrated by simulations of Segel and Perelson (1989a) that show the effect of a single memory clone on a simple model immune system. If the virgin system is only barely stable to small perturbations, then the system is so sensitive that the memory clone strongly perturbs the whole system. The effect is satisfactorily smaller in a more stable system.

It is clearly worthwhile to generalise shape space simulations to higher dimension. To this end, it is expedient to simplify further our underlying model in order to reduce calculation time. One step in this direction is taken by setting $m = 0$ in Eq. (1.1). This permits use of $B = \ln b$ as a dependent variable, with consequent great reduction in stiffness. Another large saving in computation time is achieved by restricting field calculations to a fixed finite radius of the exactly complementary clone. Figure 4 depicts the results of a simulation for a two-dimensional circular shape space. Patterns of high and low populations are seen, which are reminiscent of patterns seen in reaction-diffusion equations as well as other interaction-redistribution equations (Levin and Segel, 1985).

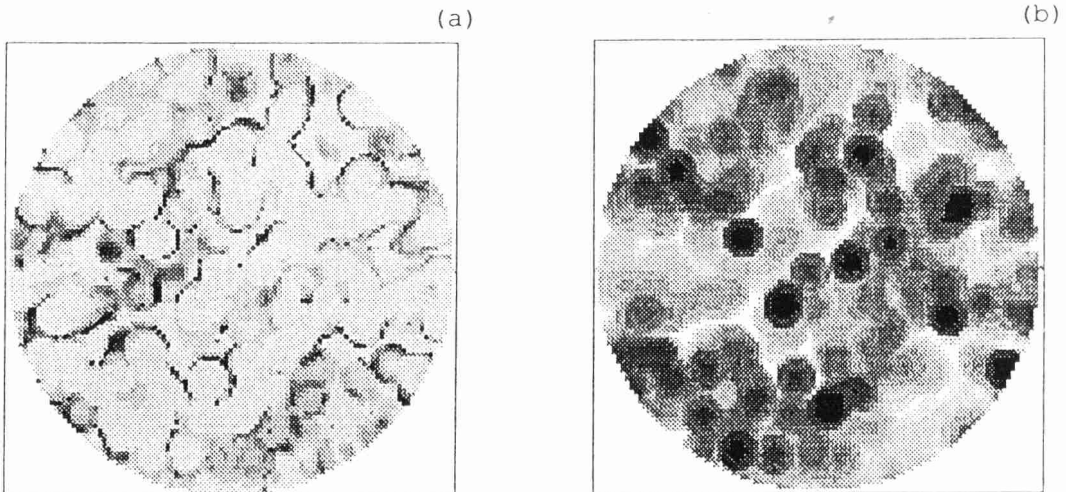


Fig.4 A 2-D pattern in shape space. The population size (a) and the field size (b) are indicated by grey scales. White corresponds to minimum values, here zero, and black corresponds to maximum values. The shape runs from $(-N, -N)$ in the bottom left corner to (N, N) in the top right corner. The population with shape $(0, 0)$ is located in the centre of the circle. The 2-D distribution of populations sizes in panel (a) forms

lines and circles that are located at intermediate values of the fields in panel (b). The standard deviation of Eq. (3.2) is $\sigma = 10\%$ of the shape space. The size of the patterns scales with σ (De Boer *et al.*, 1992).

Of particular immunological interest is the fact that a number of clones are little removed from the virgin state, and are thus "disconnected" from the network of strongly interacting clones. Coutinho (1989) and Holmberg *et al.* (1989) suggest that perhaps 80-90% of clones in mice are disconnected and thus can respond as virgin clones to foreign antigens. However, only about 5% of the clones were disconnected in one-dimensional shape space simulations. This is very far from a result that is reasonable either on grounds of abstract ideas of efficiency or on grounds of agreement with experiment. Yet the percentage of disconnected clones typically doubled in two-dimensional simulations (De Boer *et al.*, 1992). There is thus strong motivation to extend the model results to higher dimension. Whether done analytically or numerically, this offers a strong challenge for the future.

4. Variable Network Compositions

The main advantage of the two models discussed so far is that their simplicity allows for mathematical analysis. Thus, in the shape space model we have been able to analyse the stability of the three homogeneous steady states of the model to uniform and sinusoidal perturbations (De Boer *et al.*, 1992). In the Cayley tree model we have been able to find conditions for the existence of localised attractors (Weisbuch *et al.*, 1990). By further simplification of the Cayley tree model to a window automaton we have been able to analyse the conditions for attaining the steady states (Neumann and Weisbuch, 1991a).

A major disadvantage of the two models discussed so far is that they ignore the turnover of clones in the network. In the immune system the bone marrow produces novel clones with new receptors at a rate that is sufficient to replace all clones in the network in a few days. Thus, it seems that in the network the addition and deletion of clones takes place on a similar time scale as the growth and decay of B cell populations. This aspect of the immune system was first considered in the simulation model of Farmer, Packard and Perelson (1986). Farmer *et al.* (1987) as well as Varela *et al.* (1988) have used the term "meta-dynamics" for the change in dynamics of the system owing to the replacement of clones in the network. By adding a form of meta-dynamics to our model we have attempted to account for the effects of clonal insertion and deletion processes in the network (De Boer and Perelson, 1991).

Another feature of the immune network that is not exhibited by the simpler models is the fluctuating behavior of individual clones. Experimental data indicate that antibody concentrations fluctuate on a time scale of about two weeks. It has been suggested that these fluctuations may be chaotic (Lundkvist *et al.*, 1989; Varela *et al.*, 1991). Our models also yield oscillatory or chaotic behavior if we make them more realistic by splitting b_i into a B cell population B_i and an antibody population A_i of the same specificity. Differences in the time scales of B cell and antibody life times are responsible for this new form of behavior (De Boer and Hogeweg, 1989b;

De Boer *et al.*, 1990; De Boer and Perelson, 1991; De Boer, Kevrekidis, and Perelson, submitted; Perelson and Weisbuch, 1991). Oscillatory behavior has also been found in similar models of the immune network (Varela *et al.*, 1988; Stewart and Varela, 1989, 1990).

We studied the general properties of a network that incorporated meta-dynamics and contained both B cells and antibodies (De Boer and Perelson, 1991). Because the immune network seems to be most significant during early life (Coutinho, 1989; Holmberg *et al.*, 1989) we also studied the model as it develops and acquires structure as it adds more and more clones. Immunologists call this the *selection of the immune repertoire*. We are interested in emergent properties like the size and the connectivity of the network as a function of the model parameters.

4.1. The Model

The De Boer and Perelson (1991) model is composed of a varying number of B cell clones of different specificities that form a network. A source, intended to model the bone marrow, supplies novel B cell clones that can be incorporated into the network. Each clone is characterised by its specific antibody receptor, which is specified in the model by a bit-pattern that reflects the "shape" of the antibody (cf. Farmer *et al.*, 1986). Two clones can interact via solution phase antibodies whenever their receptor shapes (i.e., bit-patterns) are complementary. Cells that become activated, proliferate and differentiate into antibody secreting cells. This maturation process takes a few days. Free antibodies may also react with complementary antibodies to form *complexes*. These complexes, which are analogous to antigen-antibody complexes, are removed from the system at a certain rate.

The field of a clone is defined as in (1.2). The field represents the combined effect of all the anti-idiotypic antibodies in the environment, weighted by the affinities of the various interactions. The activation function $f(h_i)$ is the log bell-shaped function introduced in (1.4).

To model the dynamics of the various B cell clones we consider that cells proliferate at rate p upon idiotypic stimulation, and decay at rate d_B . Thus

$$\frac{dB_i}{dt} = B_i [pf(h_i) - d_B] , \quad (4.1)$$

where $f(h_i)$ is the fraction of activated B cells of type i . This differential equation differs from Eq. (1.1) in that it has no source. To model the time-dependent aspects of antibody production we introduce a "gearing up" function, $G(t)$, that accounts for the time lag associated with the differentiation of stimulated B cells. We introduce a separate gearing up function for each clone so that $G_i(t)$ can be interpreted as the proportion of mature B cells of type i . Following Segel and Perelson (1989b) we construct $G_i(t)$ as the solution of the first order differential equation

$$\frac{dG_i}{dt} = k[f(h_i) - G_i] , \quad (4.2)$$

where $f(h_i)$ is the activation function and k is a constant that determines the characteristic time for gearing up. At $t=0, G_i(0)=0$ so that there is no initial secretion. After antibodies are secreted they are free in solution. Free antibodies can form complexes with complementary antibodies and be eliminated at rate d_C . Additionally, antibodies decay at rate d_A . Thus

$$\frac{dA_i}{dt} = sB_iG_i - d_C A_i h_i - d_A A_i, \quad (4.3)$$

where s is the rate at which a fully mature B cell produces antibody. The formation of an antibody-antibody complex is a reversible reaction, which typically reaches equilibrium rather rapidly. In equilibrium the concentration of $A_i - A_j$ complex is $J_{ij} A_i A_j$. Thus the coefficient d_C multiplies the equilibrium concentration of all possible complexes, $A_i h_i$.

To summarise, our model consists of $3N$ differential equations, where N is the number of clones in the system. The size of the network N is determined by the meta-dynamics.

4.2. Meta-dynamics

The shape of each antibody molecule is represented as a bit-string of length L , see also (Farmer *et al.*, 1986; Perelson, 1988; De Boer and Hogeweg, 1989b). Antibody molecules are assumed to recognise each other whenever their bit-strings can be matched complementarily. The specific rule that we apply here is that we align the bit-strings and require a complementary match over a stretch of at least T adjacent positions. If the strings match over exactly T adjacent positions, we assign a low affinity, i.e., $J_{ij} = 0.1$. Whenever the strings match over more than T adjacent positions, we assign a high affinity, i.e., $J_{ij} = 1$. We set $L = 32$ and vary T in order to vary the matching probability $P(\text{match})$ of the receptors. In fact, for our specific match rule, $P(\text{match})$ is the probability of finding a "success run" of length T in a sequence of L Bernoulli trials (e.g., T "heads" in a row in a sequence of L coin tosses). Feller (1968) provides an approximate formula for $P(\text{match})$ that becomes reasonably accurate for $L \geq 2..$ Using Feller's result we find for $L = 32$ and $T = 6, 7, 8, 9, 10,$ and 11 , $P(\text{match}) = 0.205, 0.103, 0.05, 0.024, 0.012,$ and 0.005 , respectively. Experimental data suggest that during early life, clones are on average connected to 20-25% of the clones in the network (Holmberg *et al.*, 1984; Kearney *et al.*, 1987). For $L = 32$ such a connectivity, i.e., $P(\text{match}) \approx 0.2$, is expected around $T = 6$.

From the genetics of antibody V region gene recombination, it seems that the potential repertoire should be much greater than the repertoire present in the B cells of an organism at any one time. Because of this large discrepancy in repertoire sizes, we shall assume that each time a clone is generated in the bone marrow it contains a unique antibody variable region, i.e., a unique bit-string, that is produced for the first time. Thus, we assume that M novel clones are produced daily, with each clone

containing about 10 cells. Using the string matching algorithm, we compare each newly generated clone with all other clones already existing in the network. A new clone is incorporated in the network only if it recognises at least one other clone already present in the network - and if these interactions are sufficiently stimulatory so that the clone is expected to increase following its introduction (i.e., $dB_i / dt > 0$). At time intervals of one day, all clones in the model are checked for the size of the B cell and antibody population. If $B_i < 1$ and $A_i < \theta_1 / 10$, i.e., if the clone consists of less than one cell, and if its antibody population is too small to have any effect, then the clone is removed from the network. As an initial condition we start with a few randomly generated antibodies, assumed to represent maternal antibodies. See De Boer and Perelson (1991).

4.3. Results

Figure 5 shows the variation in time of some global characteristics of a sample network for several values of the clonal production rate (i.e., $M = 10, 20, 40$; lines increase in thickness with M). The number of clones in the network N (Fig. 5a), has a large peak during the first month, whose height increases with M . This early peak sharply declines by the third month, and the network attains an equilibrium size

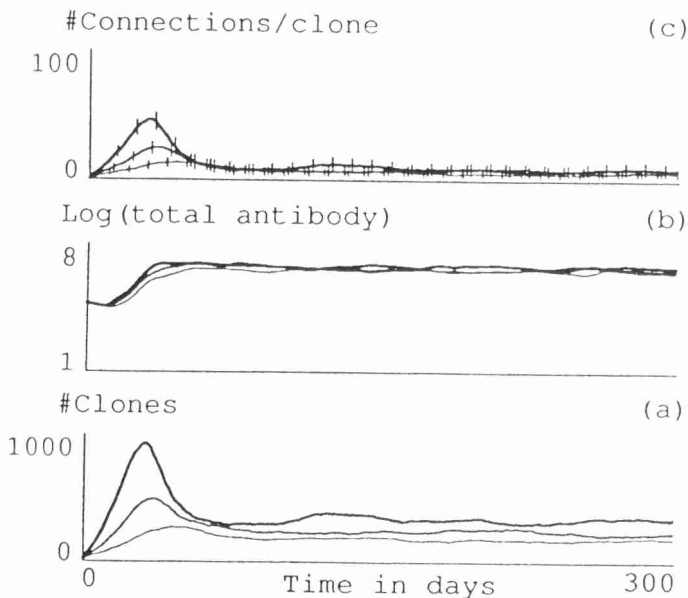


Fig.5 Time dependent characteristics of a sample network. Parameters $p=1, d_B=0.5, d_A=0.05, s=1, d_C=10^{-3}, \theta_1=10^2, \theta_2=10^4, k=0.2, T=8, P(\text{match})=0.05$. We show three values of bone marrow production: $M=10, M=20$, and $M=40$. Lines increase in thickness with M . (a) The number of clones in the network, (b) the total antibody on a logarithmic scale (base ten), and (c) the average connectivity. (The bars indicate one standard deviation).

around which it fluctuates. The total amount of antibody produced by the network is shown in Fig. 5b. After a slow decline of the maternal antibodies, the total antibody concentration increases until a steady state level of about 3×10^6 units is attained. The daily average number of connections per clone, i.e., the connectivity of the network, is shown in Fig. 5c. As in Fig. 5a, Fig. 5c shows an early peak and attains an equilibrium around day 100. This equilibrium is about 6-9 connections per clone.

The explanation for the initial peak in the number of clones and in the connectivity is found in the antibody concentrations (see Fig. 5b). When the system has not yet filled with antibody, the antibody population of each clone is small. Thus the stimulation of each individual clone requires the interaction with many anti-idiotypic clones. The fact that equilibrium levels are attained in Fig. 5 shows that the idiotype network has certain self-structuring properties: the network selects a certain size, connectivity, and antibody level. The stable properties are surprising since each individual member of the network oscillates and because the individual members are continuously being renewed. These self-structuring properties are further investigated below by analysing a series of networks in which $P(\text{match})$ is varied.

The three self-structuring properties of the network are plotted, in Fig. 6, as a function of $P(\text{match})$ for three different values of the bone marrow supply rate M . The equilibrium size of the network strongly depends on $P(\text{match})$ (Fig. 6a). Networks comprised of sticky receptors (e.g., $P(\text{match}) > 0.1$) remain very small and contain fewer than 200 clones. Conversely, whenever receptors are specific (e.g., $P(\text{match}) < 0.01$), the networks become very large. From the shape of the observed curves we

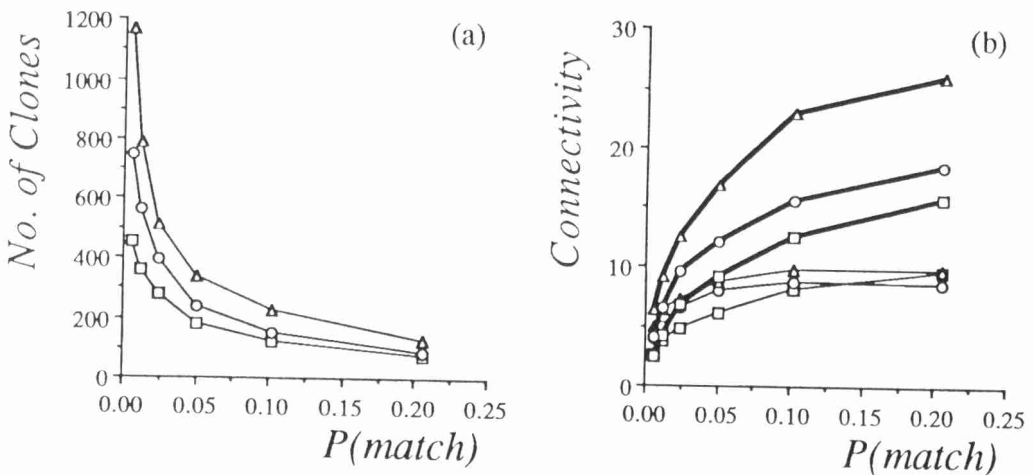


Fig. 6 Characteristics of a series of networks varying $P(\text{match})$. Parameters as in Fig. 5. The equilibrium values were determined by averaging over the last 100 time steps of a simulation. We show three values of M : $M = 10$: Δ , $M = 20$: \circ , $M = 40$: \square . (a) The total number of clones (light lines). (b) The network connectivity (light lines), and the expected network connectivity (heavy lines).

conclude that the number of clones is inversely related to $P(\text{match})$. Thus, systems with highly specific receptors will generate very large networks.

The light lines in Fig. 6b depict the network connectivity, i.e., the average number of connections per clone. For low values of $P(\text{match})$ the connectivity increases with $P(\text{match})$ until it saturates at about 10 connections per clone. This saturation is surprising because it means that the connectivity no longer depends on the matching probability. It shows that one cannot deduce $P(\text{match})$ from the connectivity data. The experimental estimate of a connectivity of 20-25% is only a transient in this model, which is attained during the early peak shown in Fig. 6.

The "expected connectivity" of a network, i.e., the $P(\text{match})$ multiplied by N , the number of clones in the network (as provided in Fig. 6a), is shown by the heavy lines in Fig. 6b. Because the connectivity is always smaller than the expected connectivity, we conclude that the networks are selecting for low connectivity.

The fact that the observed equilibrium size of the networks is inversely related to $P(\text{match})$ accounts for a "self-regulatory completeness" of the repertoire: the higher the specificity of the receptors the larger the number of clones becomes in the immune network, so that the repertoire remains complete. This completeness also provides an explanation for the fact that the networks attain an equilibrium size. The networks grow until every bit string is expected to be connected to a sufficient number of other clones to remain stimulated. The original paper of De Boer and Perelson (1991) explains this in more detail.

The incorporation of meta-dynamics in this model was an attempt to account for the rapid turnover of clones in the immune network. Unfortunately, due to computational problems, it is impossible in this model to perform the simulations for the correct time-scale of the meta-dynamics. In the immune system the bone marrow produces of the order of $M = 10^5$ to $M = 10^6$ novel clones per day. In our simulations we have gone up to $M = 500$ (De Boer and Perelson, 1991). Thus, it is unknown whether our results really apply to immune networks with such a rapid turnover of clones. In an attempt to meet this difficulty, we have simplified the 2D shape space model (De Boer *et al.*, 1992) using the window automaton proposed by Neumann and Weisbuch (1991) and have implemented this as a cellular automaton (work in progress). In this formalism it becomes possible to study the correct time scale of bone marrow production.

4.4. Conclusions

We have derived the following main conclusions for our model network. The equilibrium size of the idiotypic network is a property that emerges from interactions among the clones in a network. It is inversely related to the matching probability of immunoglobulin receptors. This dependence of size on specificity accounts for a form of "self-regulatory completeness." Networks grow large enough so that their repertoires are complete. Once a network is established it selects an immune repertoire. The number of clones in the network is much smaller than the total number of clones supplied by the bone marrow. The clones that survive, form the network and influence the immune repertoire. The connectivity of the network,

defined as the average number of connections per clone, is another emergent property and is relatively independent of the matching probability of the receptors. The number of different clones in the network and their connectivity is very large during the first month and then decreases later in life. Networks select for clones with few connections. The population size of most clones in the network fluctuates in time. Nevertheless, the network as a whole attains a number of constant equilibrium properties.

5. Discussion

The most important difference between the three approaches outlined in this review is our result that attractors tend to be localised in the Cayley tree networks of Section 2, but tend to be distributed in the shape space networks of Section 3 and the variable composition networks of Section 4. Since the networks studied in Section 3 and 4 do not obey the Cayley tree topology of Section 2, the different results may be due to the different topologies. However, since some of the modifications of the Cayley tree topology allow for the existence of localised attractors (Neumann and Weisbuch 1991b), the difference in the results can also be due to differences in dynamical regimes and/or in initial conditions. This requires further study.

From an immunological perspective it is also unclear whether or not one should expect the attractors of the immune network to be localised or distributed. The experimental data cited in this paper (Coutinho, 1989, Holmberg *et al.*, 1989, Lundkvist *et al.*, 1989; Varela *et al.*, 1991) suggest network properties to be distributed. However, because most of these data were obtained in young animals this need not be true for adult immune systems.

Thus, the best approach to this problem seems to be a variety of approaches that are based upon different assumptions. In this review we have outlined three of them.

Acknowledgements

GW and AUN thank H. Atlan and B. Derrida for helpful discussions. The Laboratoire de Physique Statistique is associated with CNRS (URA 1306); financial support was received from Inserm grant 879002 and a NATO Collaborative Research Grant. AUN is supported by an Inserm Fellowship. ASP and LAS acknowledge support from the U.S. - Israel Bi-national Science Foundation, Grant 89-00146. ASP, RdB and LAS acknowledge support from NIH Grants RR06555 and AI28433. The work of ASP was performed under the auspices of the U.S. Department of Energy.

References

1. Coutinho, A. (1989) *Immunol. Rev.*, **110**:63-87.
2. De Boer, R. J. (1983) *GRIND: Great Integrator Differential Equations.*, *Bioinformatic Group, University of Utrecht, The Netherlands.*

3. De Boer, R. J. (1988) In *Theoretical Immunology, Part Two* (A.S. Perelson, ed.), vol. 3 in *SFI Studies in the Science of Complexity*. Addison-Wesley, Redwood City, CA: pp. 265-289.
4. De Boer, R. J. and P. Hogeweg. (1989a) *Bull. Math. Biol.*, **51**:223-246.
5. De Boer, R. J. and P. Hogeweg. (1989b) *Bull. Math. Biol.*, **51**:381-408.
6. De Boer, R. J. and P. Hogeweg. (1989c) *J. Theoret. Biol.*, **139**:17-38.
7. De Boer, R. J., I. G. Kevrekidis, and A. S. Perelson. (1990) *Chem. Eng. Sci.*, **45**:2375-2382.
8. De Boer, R. J. and A. S. Perelson. (1991) *J. Theoret. Biol.*, **149**:381-424.
9. De Boer, R. J., L. A. Segel, and A. S. Perelson. (1992) *J. Theoret. Biol.*, **155**: 295-353.
10. Farmer, J. D., N. H. Packard, and A. S. Perelson. (1986) *Physica D***22**:187-204.
11. Farmer, J. D., S. A. Kauffman, N. H. Packard, and A. S. Perelson. (1987). *Annals New York Acad. Sci.* **504**:118-130.
12. Feller, W. (1968) *An Introduction to Probability Theory and its Applications* Volume 1: Third Edition, Wiley, NY, pp. 323-326.
13. Holmberg, D., A. Andersson, L. Carlson, and S. Forsgen. (1989) *Immunol. Rev.*, **110**:89-103.
14. Kearney, J. F., M. Vakil, and N. Nicholson. (1987) In *Evolution and Vertebrate immunity: the antigen receptor and MHC gene families*, G. Kelsoe and D. Schultze, eds, *Texas University Press*, Austin, pp. 373-389.
15. Hopfield, J. J. (1982) *Proc. Natl. Acad. Sci. USA.*, **79**:2554-2558.
- Jerne, N. K. (1974) *Ann. Immunol. (Inst. Pasteur)*, **125** C:373-389.
- Levin, S. A. and L. A. Segel. (1985) *SIAM Rev.*, **27**:45-67.
16. Lundkvist, I., A. Coutinho, F. Varela, and D. Holmberg. (1989) *Proc. Nat. Acad. Sci. USA.*, **86**:5074-5078.
17. Neumann, A.U. and G. Weisbuch. (1991a) *Bull. Math. Biol.* **53**: 21-44
18. Neumann A.U. and G. Weisbuch. (1991b) *Bull. Math. Biol.* **53**: 699-726
19. Perelson, A. S. (1984) In *Cell Surface Dynamics: Concepts and Models* (A. S. Perelson, DeLisi, C. and Wiegel, F. M., eds.). *Marcel Dekker*, New York, pp. 223-276.
20. Perelson, A. S. (1988). *Theoretical Immunology, Part Two*, A. S. Perelson, ed. Vol. 3 of *SFI Studies in the Science of Complexity*. Redwood City, CA: Addison-Wesley, pp. 377-401.
21. Perelson, A. S. (1989) *Immunol. Rev.*, **110**:5-36.
22. Perelson, A. S. and G.F. Oster. (1979) *J. Theoret. Biol.* **81**:645-670.
23. Perelson, A. S. and C. DeLisi. (1980) *Math. Biosci.*, **48**:71-110.
24. Perelson, A. S. and G. Weisbuch. (1991). *Bull. Math. Biol.* (in press).
25. Segel, L. A. and A. S. Perelson. (1988) In: *Theoretical Immunology, Part Two*, A. S. Perelson, ed. Vol. 3 of *SFI Studies in the Science of Complexity*. Redwood City, CA: Addison-Wesley, pp. 321-343.
26. Segel, L. A. and A. S. Perelson. (1989a) In: *Theories of Immune Networks*, ed., Atlan, H., *Springer-Verlag*, Berlin, pp. 63-70.
27. Segel, L. A. and A. S. Perelson. (1989b) In: *Theoretical Models for Cell to Cell Signalling*, ed., Goldbeter, A., *Academic Press*, New York, pp. 261-272.
28. Segel, L. A. and A. S. Perelson. (1990) *Siam J. Appl. Math.* **50**:91-107.
29. Stewart, J. and F. J. Varela. (1989) *Immunol. Rev.*, **110**:37-61.
30. Stewart, J. and F. J. Varela. (1990) *J. Theoret. Biol.*, **144**:103-115.

31. Stewart, J. and F. J. Varela. (1991) *J. Theoret. Biol.*, In press.
32. Varela, F. J., A. Coutinho, B. Dupire, and N. N. Vaz. (1988) In *Theoretical Immunology, Part Two* (A.S. Perelson, ed.), vol. 3 of *SFI Studies in the Science of Complexity*. Redwood City, CA: *Addison-Wesley*, pp. 359-375.
33. Varela, F. J. and A. Coutinho. (1991) *Immunology Today*, **12**:159-166.
34. Varela, F. J., A. Anderson, G. Dietrich, A. Sundblad, D. Holmberg, M. Kazatchkine, and A. Coutinho. *Proc. Nat. Acad. Sci. USA* In press.
35. Weisbuch, G. (1990) *J. Theoret. Biol.*, **143**:507-522.
36. Weisbuch, G., R. J. De Boer, and A. S. Perelson. (1990) *J. Theoret. Biol.*, **146**:483-499.
37. Weisbuch, G. and A. U. Neumann. (1991) In *Proceedings of the Les-Houches winter School* (R. Livi, J.P. Nadal, and N.H. Packard, Eds), *North-Holland*, The Netherlands.